7TH INTERNATIONAL CONFERENCE ON STRUCTURAL ANALYSIS OF ADVANCED MATERIALS.
BOOK OF ABSTRACTS. Vol. VII, 2017. CD-ROM ISSN 2247–8337, Online ISSN 2559-7841, ISSN-L 2247–8337

Modeling the Behavior of Human Body Tissues on Penetration

A. CONCI[1,a)], A. L. BRAZIL[1,b)], D. POPOVICI[2,c)], G. JIGA[3,d)], F. LEBON[4,e)]

[1]*Computer Institute, Universidade Federal Fluminense, Niterói, Rio de Janeiro, Brazil*
[2]*Department of Electrical Engineering, University POLITEHNICA of Bucharest, Romania*
[3]*Department of Strength of Materials, University POLITEHNICA of Bucharest, Romania*
[4]*Lab. Mécanique Acoustique, Aix-Marseille Univ., CNRS, Centrale Marseille, Marseille, France*

[a)]aconci@ic.uff.br
[b)]andrelbrazil@yahoo.com
[c)]dorina.popovici25@gmail.com
[d)]gabijiga@yahoo.com
[e)]lebon@lma.cnrs-mrs.fr

Abstract. Several procedures in medicine (such as anesthesia, injections, biopsies and percutaneous treatments) involve a needle insertion. Such procedures operate without vision of the internal involved areas. Physicians and anesthetists rely on manual (force and tactile) feedback to guide their movements, so a number of medical practice is strongly based on manual skill. In order to be expert in the execution of such procedures the medical students must practice a number of times, but before practice in a real patient they must be trained in some place and a virtual environment, using Virtual Reality (VR) or Augmented Reality (AR) is the best possible solution for such training. In a virtual environment the success of user practices is improved by the addition of force output using haptic device to improve the manual sensations in the interactions between user and computer. Haptic devices enable simulate the physical restriction of the diverse tissues and force reactions to movements of operator hands. The trainees can effectively "feel" the reactions to theirs movements and receive immediate feedback from the actions executed by them in the implemented environment. However, in order to implement such systems, the tissue reaction to penetration and cutting must be modeled. A proper model must emulate the physical sensations of the needle action in the skin, fat, muscle, and so one, as if it really done in a patient that is as they are holding a real needle and feeling each tissue resistance when inserting it through the body. For example an average force value for human skin puncture is 6.0 N, it is 2.0 N for subcutaneous fat tissue and 4.4 N for muscles: this difference of sensations to penetration of each layers trespassed by the needle makes possible to suppose the correct position inside the body. This work presents a model for tissues before and after the cutting that with proper assumptions of proprieties can model any part of human body. It was based on experiments and used in embryonic system for epidural anesthesia having good evaluation as presented in the last section "Preliminary Results".

ICSAAM 2017

Organized by:

UNIVERSITY POLITEHNICA OF BUCHAREST
Faculty of Engineering and Management of Technological Systems

In collaboration with:

UNIVERSITY OF PATRAS – Mechanical and Aeronautical Department, Patras, GREECE

INSTITUTE OF SCIENCE AND INNOVATION IN MECHANICAL AND INDUSTRIAL ENGINEERING, Porto, PORTUGAL

SECOND UNIVERSITY OF NAPLES – Scientific and Technology of Materials, Naples ITALY

PUBLISHER:
University POLITEHNICA of Bucharest
Address: 313, Splaiul Independenţei, District 6, Zip code 060042, Bucharest, Romania
Phone: + 40 723 320 535
E-mail: icsaamconference@gmail.com
Web: www.icsaam.eu

To be cited: International Conference on Structural Analysis of Advanced Materials, Vol. VII, 2017

ISSN CD-ROM 2247–8337; ISSN Online 2559-7841; ISSN-L 2247–8337

Modeling the behavior of human body tissues on penetration

A. Conci, A. L. Brazil, D. Popovici, G. Jiga, F. Lebon

Keywords: Biomechanic, haptic device, in vivo, elastic, plastic, force displacement relation.

Abstract. Several procedures in medicine (such as anesthesia, injections, biopsies and percutaneous treatments) involve a needle insertion. Such procedures operate without vision of the internal involved areas. Physicians and anesthetists rely on manual (force and tactile) feedback to guide their movements, so a number of medical practice is strongly based on manual skill. In order to be expert in the execution of such procedures the medical students must practice a number of times, but before practice in a real patient they must be trained in some place and a virtual environment, using Virtual Reality (VR) or Augmented Reality (AR) is the best possible solution for such training. In a virtual environment the success of user practices is improved by the addition of force output using haptic device to improve the manual sensations in the interactions between user and computer. Haptic devices enable simulate the physical restriction of the diverse tissues and force reactions to movements of operator hands. The trainees can effectively "feel" the reactions to theirs movements and receive immediate feedback from the actions executed by them in the implemented environment. However, in order to implement such systems, the tissue reaction to penetration and cutting must be modeled. A proper model must emulate the physical sensations of the needle action in the skin, fat, muscle, and so one, as if it really done in a patient that is as they are holding a real needle and feeling each tissue resistance when inserting it through the body. For example an average force value for human skin puncture is 6.0 N, it is 2.0 N for subcutaneous fat tissue and 4.4 N for muscles: this difference of sensations to penetration of each layers trespassed by the needle makes possible to suppose the correct position inside the body. This work presents a model for tissues before and after the cutting that with proper assumptions of proprieties can model any part of human body. It was based on experiments and used in embryonic system for epidural anesthesia having good evaluation as presented in the last section "Preliminary Results".

1- Introduction:

Haptic devices enable to simulate translational and rotational restrictions and reactions in terms of forces and moment realized by operator hands. The user can effectively "sense" the reactions to his movements by receiving immediate force feedback from actions executed by the device in a computer environment. Haptics are used in a wide range of applications, including 3D modeling and realistic simulations which also comprehends medical procedures, among others. Such devices enable to experiment sensations of tissue resistances (if properly modeled) when practicing the procedures with them. It helps to identify the transitions among tissue layers and organs, as well as their nature and properties. The interaction between the medical equipment that is simulated by the haptic (e.g. needles and bistouries) and tissues can support the understanding of stiffness, cutting and friction mechanisms involved on a needle insertion procedure, improving the degree of realism on virtual simulations by emulating what physically happens on it. Movement on the simulator is transformed by input data by these devices depending of the equipment used, for instance the Phantom Omni device (Figure 1) allows six (6) degrees of freedom (DOF) and has an extremity allowing simulation of the needle rotations around the x, y and z axis by 3 gimbals. This model presents an extremity that looks like a pen (Figure 1-right) with 2 buttons. Such an extremity can represent the movement in x, y, and z axis, as 3 displacements and 3 rotations in orthogonal directions (6 DOF), each one going from completely free to completely restricted, passing by some partially restriction in any degree, with correspondent forces and moments feedback related to them if computationally modeled. The moments feedback are provided by angular movements on the elements with label "rotation", identified by numbers 1 to 3 on Figure 1. The elements with label "gimbal" represent free rotation of the haptic, i.e. without possible reaction on the implementation. The combination of all these possibilities allows a proper simulation of a real procedure by the haptic in response of the user movement. Of courses other models of haptic devices are available with less DOF and low cost, as well as more complex equipments.

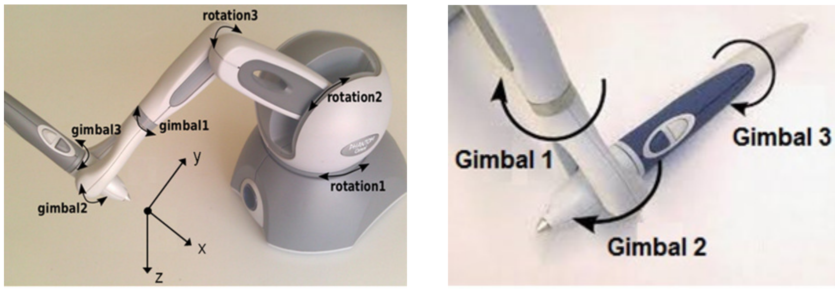

Figure 1. The Phantom Omni haptic with 6 degrees of freedom (DOF) and its extremity with a pointer with 2 buttons pointer and more 3 DOF (gimbals) (right).

2- One Layer Force Model

A simplified scheme of events on the needle insertion procedure can be visualized on Figure 2, where number 1 represents the needle and the skin before contact, when no force appears. In 2, the needle contacts the skin surface pressing it, changing the surface curvature in this point before perforation of the tissue, this contact is completely reversible, so elastic, producing a stiffness force **(S_f)**. After the applied force reaches the elastic limit, the skin perforation occurs and the behavior is no more elastic for this layer, although, it continues elastic for the subsequent layers of body tissues. Number 3 on Figure 2 represents the forces in the needle after penetration into the skin. There are two forces now, a friction **(F_f)** and a cutting **(C_f)** force, until a new tissue is reaches by the needle tip producing again an elastic reaction until surface perforation and the repetition of the process with penetration of the needle into the various tissues of the body.

The one layer force model based on combinations of stiffness, friction and cutting forces can be represented by equation (1). This model is used to represent needle insertions in soft tissues based on comparisons with anesthetized living swine [1] and experiments in bovine livers [2], and already used in works [3,4]. In such a model the applied force (**A_f**) must be superior to the resulting force (**R_f**) in order to move the needle. The resulting force (**R_f**) is considered as having 2 possibilities: before perforation due to **S_f** or after perforation due to **F_f** and **C_f** forces (1):

$$\mathbf{R}_f = \mathbf{S}_f \qquad \textbf{or} \qquad \mathbf{R}_f = \mathbf{C}_f + \mathbf{F}_f \tag{1}$$

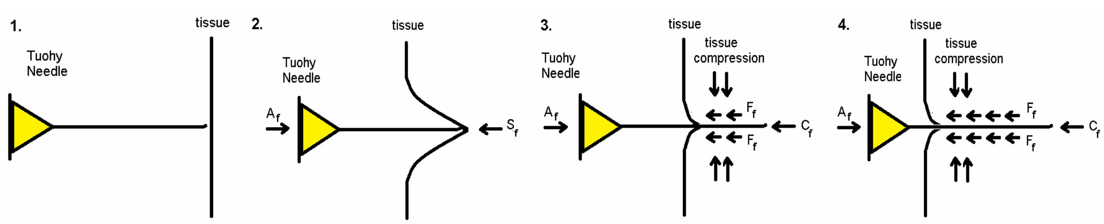

Figure 2. Simplified stages of the main forces on a needle insertion of the proposed model

The stiffness force (**S_f**) is the first to occur; it increases from zero and produces elastic deformation in the skin surface as showed in number 2 of Figure 2, before the applied force (**A_f**) be greater than elastic limit or the force to pierce the skin. Then, the needle moves into internal tissues with friction and cutting forces **($F_f + C_f$)** up they reach their maximum values or new tissue surface (number 4 in Figure 2). The cutting force (**C_f**) is related to the tissue cutting resistance while being ripped by the needle advancement and produced when the tip of the needle pierces the tissue. The friction force **(F_f)** is related to the dynamic friction caused by the needle movement inside the patient tissue. $\mathbf{F_f}$ acts on the needle surface as reaction to needle movements, due to the contact of the internal skin layer, caused by the needle shaft rubbing on the already trespassed tissue.

The coordinates of the first needle contact $\boldsymbol{P_{contact}} = (\boldsymbol{X_{contact}}, \boldsymbol{Y_{contact}}, \boldsymbol{Z_{contact}})$ determines a point on the skin surface in the model. The current haptic/needle tip position $\boldsymbol{P_{tip}}$ is define by the coordinates: $(\boldsymbol{X_{0tip}}, \boldsymbol{Y_{0tip}}, \boldsymbol{Z_{0tip}})$. Initially, $\boldsymbol{P_{contact}}$ and $\boldsymbol{P_{tip}}$ are the same point, the distance between them is represented by Δ, considering the 3D coordinates, it is $(\boldsymbol{\Delta_x}, \boldsymbol{\Delta_y}, \boldsymbol{\Delta_z})$. There is not penetration or force applied on the skin when $(\boldsymbol{X_{tip}}, \boldsymbol{Y_{tip}}, \boldsymbol{Z_{tip}}) = (\boldsymbol{X_{contact}}, \boldsymbol{Y_{contact}}, \boldsymbol{Z_{contact}})$ but at each time the user move the haptic tip the coordinates are actualizes to a new $(\boldsymbol{X_{tip}}, \boldsymbol{Y_{tip}}, \boldsymbol{Z_{tip}})$, and $\boldsymbol{\Delta} = (\boldsymbol{X_{tip}}-\boldsymbol{X_{contact}}, \boldsymbol{Y_{tip}}-\boldsymbol{Y_{contact}}, \boldsymbol{Z_{tip}}-\boldsymbol{Z_{contact}})$ is computed. The needle displacement in z axis direction, $\boldsymbol{\Delta_z}$, is related with the forces model. The $\boldsymbol{X_{contact}}$ and $\boldsymbol{Y_{contact}}$ are important to determine the internal elements to be displayed but they do not produce reactions to them in the axial model.

3- Needle Insertion Experiments

For success of needle insertion model, experimental observation of the tissues behavior is critical. This section presents some experimental works to justify the multiple layer model proposed. Needle insertion experiments on a cylindrical sample of silicone rubber (10 cm diameter and 4 cm height) with stiffness properties similar to bovine liver was used as phantom for mapping velocity in tissue penetration of stainless-steel needle of various diameters and tip types [2]. The graphs of Figure 3 compare experiments on pregnant and non pregnant women considering epidural needle insertion, this region present the layers of tissues showed in the left image of same figure. These graphs present the stress versus the velocity in the lumbar tissues and show alternations of elastic (linear and nonlinear) and plastic behavior. The first stage, before de number 1, represents the needle sensors motion before skin insertion. There are maximum stress at the end of each layer of tissues and a sudden drop in the resistance after the star of puncture of new tissue surfaces. Letter A and number 3 show the maximum peak before entering the epidural space (ES). The droop in B is used to identify the entrance in the ES and C is the pressure after catheter insertion. Higher stress (85 kPa) appears for non-pregnant women (against 50 kPa for pregnant ones) [5].

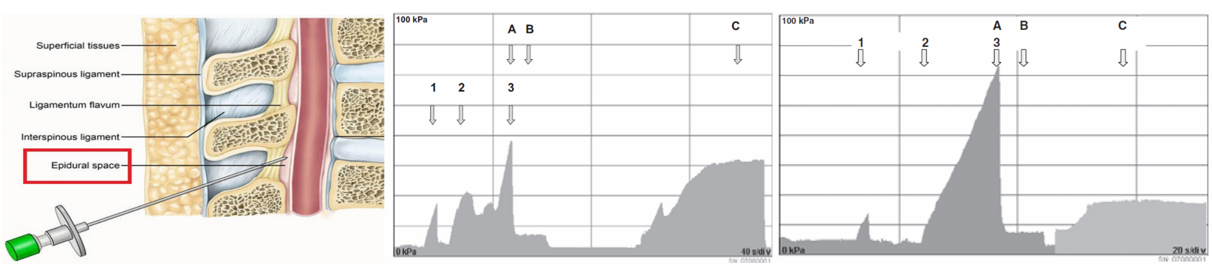

Figure 3. Tissues of epidural region (left): Superficial tissues are composed by skin (S), muscle (M) and fat tissues (FT); supraspinous ligament (SL) , interspinous ligament (IL); flavum ligament (FL) , epidural space (ES) and bones (B). Average resistances (kPa) to needle insertion on pregnant (center) and non-pregnant (right) women showing the pre e pos puncture behavior of each tissue of the region according experiments [5].

Force displacement functions for each tissue in epidural needle insertions are proposed based on needle puncture experiments on fresh porcine cadavers, human skin and fat tissues tested in a MTS machine [6]. Needle insertions speed was 0.2 mm/s. Results are compared with high-resolution MR images to improve tissue identifications [6]. They are plotted in Figure 4 showing the curve for epidural needle insertion in average woman considering all tissues of the region Figure 3-left. Note that there are plastic behaviors (i.e. an increase of displacement without increase of stress or force) after the puncture for some tissues. Experiments resulting on Figure 4 did not consider the influence of needle insertion speed, needle deflection and initial insertion angles [6].

4- Multi Layer Force-Displacement Model

Based on the experiments reported in last section, we suggest a multi layer model based on three stages: pre-puncture, on-puncture and post-puncture, using the three types of forces for the different tissues (**S_f, F_f** and **C_f)** to compute the total reaction transmitted from the haptic to the used, based on the needle displacement variation (**Δz**): i.e. the axial distance between the position of first needle contact with tissue (**$Z_{contact}$**) and the current needle tip position (**Z_{tip}**) [2]. As mentioned **Δ_z** is used to verify the tissue layer under consideration and its properties, like the maximum **S_f** (that represents the maximum tissue elasticity before its perforation by the needle), friction force (**F_f**) of the tissue (representing the properties of dynamic friction) and cutting force (**C_f**).

For each layer, two behaviors are identified: elastic (before perforation) and plastic (steady state after perforation or post-puncture). On-puncture there is a stop on the resistance to the motion of the needle tip under a constant level of resistance or with decline on the level of reaction, depending of the tissue in contact with the needle tip and their properties (measured by **Z** coordinates). Even the elastic stage, depending on the tissues**,** can present various behaviors from linear to nonlinear relation with this displacement [7]. To model all these possible relation between force and displacement we propose the polynomial relation (2) with eight constants for the various tissues in pre and post puncture state:

$$\mathbf{R_f} = \mathbf{C}_{i0} + \mathbf{C}_{i1}\,\Delta_z + C_{i2}\,\Delta_z^2 + C_{i3}\,\Delta_z^3 \tag{2}$$

where ***i*** can be ***e*** or ***p*** , i.e. it can represent the constant related to the **elastic** stiffness force (**S_f**) or to the **plastic** after perforation behavior (combining **F_f** and **C_f** forces directly). We suggest and have used in implementations the constants in Table 1 since they are based on the experiments reported in last section named: “Needle Insertion Experiments”[8].

Table 1. Constants to be used for the proposed equation (2) to model tissues in the epidural region.

Tissue	C_{e0} [N]	C_{p0} [N]	C_{e1} [N/mm]	C_{p1} [N/mm]	C_{e2} [N/mm2]	C_{p2} [N/mm2]	C_{e3} [N/mm3]	T_f [N]	ΔZ_t [mm]	$S_{f\,max}$ [N]
S	0.024	6.037	0.012	0.452	-0.005	-0.529	0.003	1.974	n/a	6.037
M	1.974	4.354	0.829	-2.254	0.108	0.290	0	3.675	n/a	4.354
IL	4.406	7.467	0.960	0	0	0	0	n/a	18	7.467
FL	4.533	12.133	1.503	-0.169	-0.058	-0.118	0	n/a	7.4	12.133
ES	2.437	2.437	0	0	0	0	0	n/a	8.6	2.436
B	3.974	n/a	2.210	n/a	1.481	n/a	0	n/a	10	50

For some tissues there are not experimental data, they are marked as ***non available*** (n/a). In some cases zero default values can be used, for instance this is the value of C_{p3} constant for all tissues, for this they are not included in Table 1.

In this model, the constants for a tissue used in (2) must consider all previously trespassed layers (ex.: the constant for muscle (M) contains the skin (S) resistance). The data of Table 1 are based on experiments [6], and their curve fitting to better represent all tissue in a unique equation [8]. The force versus needle displacements relation using these constants is plotted in Figure 5, where the stages before tissue puncture are represented in red lines and in green is drawn the after puncture. The names of the tissues in contact with the haptic tip are indicated by the arrows. The transition from "before puncture" to "after puncture" stage occurs by achieving tissue maximum stiffness force (**$S_{f\,max}$**), that is the last column in Table 3, or the next tissue (considering haptic Z coordinates and the tissue thickness ΔZ_t). Table 3 presents a column named T_f or tissue transition force that is used on the post puncture (plastic) behavior of each layer. After puncture but before penetration of the next tissue, the forces drop of a certain level (these values of T_f) or up to find the next layer whatever comes first. For instance, the transition from skin (S) to muscle (M) occurs when the R_f reaches the T_f (see line skin to muscle), which is 1.974 N. On the other hand, the tissue transition from flavum ligament (FL) to epidural space (ES) occurs when the Z coordinates goes to the end of this tissue (ΔZ_t=7.4 mm) i.e. all the tissue of the FL is trespassed by the needle.

5- Preliminary Results

Tissue pressure-time [9], forces-time [10], and forces-displacement [11] curves from experimentation are used to propose the presented model (2). A comparison among the experimental behavior [6] and the Multi Layer Force-Displacement Model presented in last section indicates that force x displacement function of equation (2): (a) is a simplified versions of previous work [2]; (b) presents stiffness force similar to the pre-puncture stage [6]; and (c) has the friction force [2] and the post-puncture stage as main difference from these models [6]. Some works report an ascendant force [2] due friction after tissue puncture, while others [1, 6] report a descendant one [6] due cutting force. Functions from [12] map all tissues relevant for an epidural needle insertion in a model that is also a simplified version of [6], considering a cumulative linear progression of stiffness and friction forces, represented by stiffness and damping coefficients, respectively, however, cutting forces and needle deflection were not considered.

The here proposed model is implemented in an embryonic system for training epidural anesthesia presenting "gamifications" recourses where the answer to the used movements are represented in the screen and on the haptic to the user [8]. Figure 6 presents some phases of this [8]. We have considered the system evaluated by System Usability Scale (SUS)[13]. SUS is a ten-item scale for subjective assessments of system usability resulting in a score from 0 to 100. Preliminary tests with medicine students resulted in an averaged SUS score of 73 which represents an acceptable result [13]. These students considered that the system improve their practice. As future work, we intend to get feedback from experts to validate the model and simulated sensations for continuous improvements of the model. We intend to compare sensation from the system with real patients and get feedback from physicians concerning the quality of the developed system, in order to promote continuous improvements.

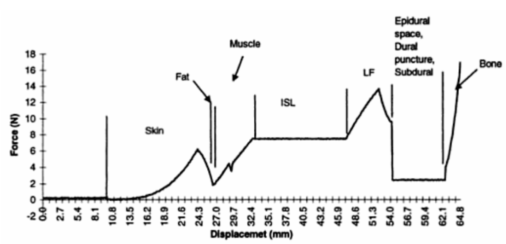

Figure 4. Force displacement of average woman [6]

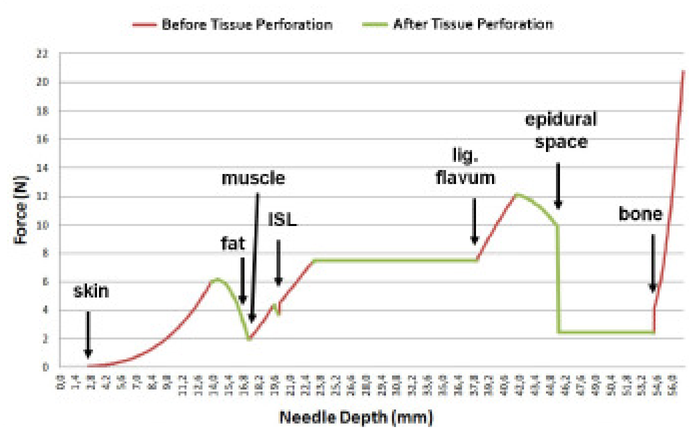

Figure 5. Force displacement using equation (2).

Acknowledgment

AC is partially supported by the CNPq Brazilian Agency, FAPERJ (projects SIADE-2 and CNE) and the LMA-UAM.

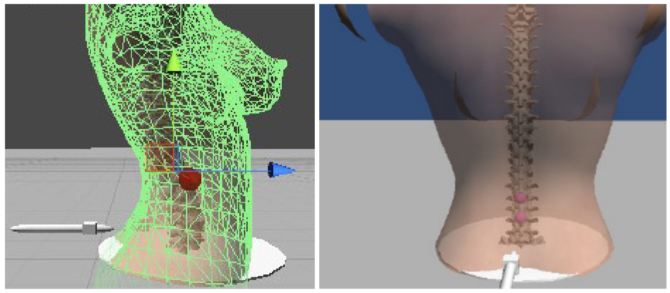

Figure 6. Some screens of the implemented system using developed equation (2) and tissues constants.

References

[1] B. Maurin, L. Barbe, B. Bayle, P. Zanne, J. Gangloff, M. De Mathelin, A. Forgione, “In vivo study of forces during needle insertions”, In: Proceedings of the Medical Robotics, Navigation and Visualisation Scientific Workshop, Ramagen, Germany (2004) 1-8.

[2] A. M. Okamura, M. C. Simone, M. Leary, “Force modeling for needle insertion into soft tissue”, IEEE Transactions on Biomedical Engineering, 51 (2004) 1707-1716.

[3] N. Abolhassani, R. Patel, M. Moallem, Needle insertion into soft tissue: A survey. Medical engineering & physics, 29 (2007) 413-431.

[4] N. Vaughan, V. N. Dubey, M. Y. Wee, R. Isaacs, “A review of epidural simulators: where are we today?” , Medical Engineering & Physics, 35 (2013) 1235-1250.

[5]T. J. M. Lechner, M. G. F. van Wijk, A. A. J. Jongenelis, M. Rybak, J. van Niekerk, C. J. M. Langenberg, The use of a sound enabled device to measure pressure during insertion of an epidural catheter in women in labour, Anaesthesia 66.7 (2011) 568-573.

[6] L. Holton, L. Hiemenz, Force models for needle insertion created from measured needle puncture data, Studies in health technology and informatics (2001) 180-186.

[7] W. Maurel, 3D modeling of the human upper limb including the biomechanics of joints, muscles and soft tissues. PhD thesis, Laboratoire d'Infographie - Ecole Polytechnique Federale de Lausanne, 1999.

[8] A.L. Brazil, An Epidural Nerve Block Simulator Using Haptics andGamification”Ph.D. thesis, Dep of computer Science, UFF, 2017.

[9]N. Vaughan, V.N. Dubey, M.Y. Wee, R. Isaacs, Parametric model of human body shape and ligaments for patient-specific epidural simulation, Artificial intel. in medicine 62 (2014) 129-140.

[10]D. S. Kwon, K. U. Kyung, S. M. Kwon, J. B. Ra, H. W. Park, H. S. Kang, K. R. Cleary, Realistic force reflection in a spine biopsy simulator. IEEE International Conference on Robotics and Automation (2001) 1358-1363.

[11] R. A. Lee. Technical development of common anesthesiology techniques; Neuraxial anesthesia and laryngoscopy for endotracheal intubation. TU Delft, Delft University of Technology, New Zealand, 2013.

[12] O. Gerovich, P. Marayong, A. M. Okamura, The effect of visual and haptic feedback on computer-assisted needle insertion. Computer Aided Surgery 9 (2004) 243-249.

[13] A. Bangor,P. Kortum, and J. Miller., "Determining what individual SUS scores mean: Adding an adjective rating scale", Journal of Usability Studies 4, 3 pp. 114-123, 2009.